AN2794
Application note

1 kW dual stage DC-AC converter based on the STP160N75F3

Introduction

This application note provides design guidelines and performance characterization of the STEVAL-ISV001V1 demonstration board.

This board implements a 1 kW dual stage DC-AC converter, suitable for use in battery-powered uninterruptible power supplies (UPS) or photovoltaic (PV) standalone systems.

The converter is fed by a low DC input voltage varying from 20 V to 28 V, and is capable of supplying up to 1 kW of output power on a single-phase AC load. These features are possible thanks to a dual stage conversion topology that includes an efficient step-up push-pull DC-DC converter, which produces a regulated high-voltage DC bus and a sinusoidal H-Bridge PWM inverter to generate a 50 Hz, 230 Vrms output sine wave. Other key features of the system proposed are high power density, high switching frequency and efficiency greater than 90% over a wide output load range

Figure 1. 1 kW DC-AC converter prototype

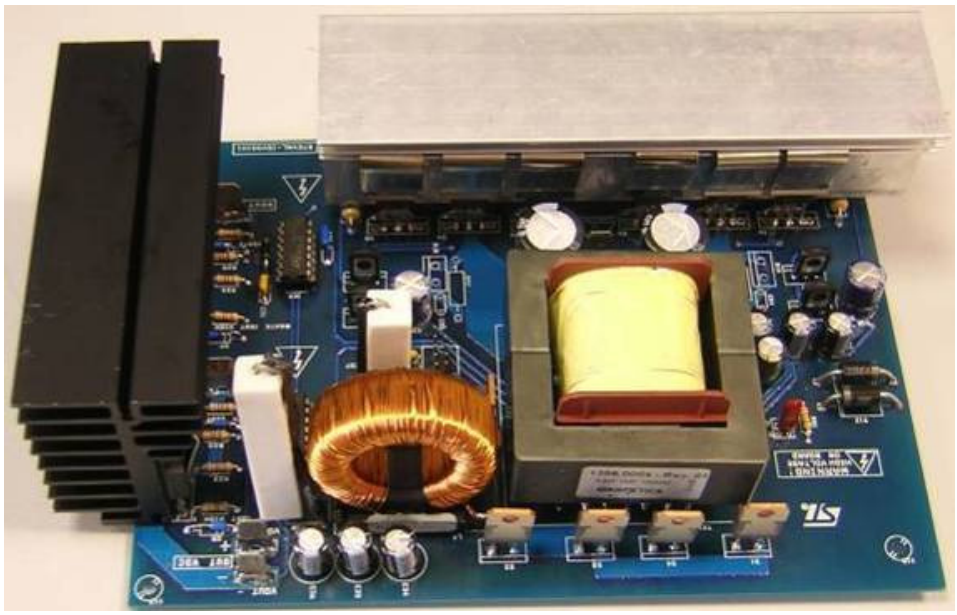

Contents

1 System description 5

2 Design considerations 8

2.1 Layout considerations 20

3 Schematic description 23

4 Experimental results 26

5 Conclusion 30

6 Bibliography 30

Appendix A Component list 31

Appendix B Product technical specification 35

7 Revision history 38

List of tables

Table 1. System specifications . . . 6
Table 2. Push-pull converter specifications . . . 9
Table 3. HF transformer design parameters . . . 13
Table 4. Output inductor design parameters . . . 16
Table 5. Power MOSFET . . . 18
Table 6. Diode . . . 18
Table 7. Bill of material (BOM) . . . 31
Table 8. Document revision history . . . 38

List of figures

Figure 1. 1 kW DC-AC converter prototype . . . 1
Figure 2. Block diagram of an offline UPS system . . . 5
Figure 3. Possible use of a DC-AC converter in standalone PV conversion . . . 5
Figure 4. Block diagram of the proposed conversion scheme . . . 6
Figure 5. Push-pull converter typical waveforms . . . 8
Figure 6. Distribution of converter losses . . . 19
Figure 7. Distribution of losses with 3 STP160N75F3s paralleled . . . 20
Figure 8. Component placement . . . 21
Figure 9. Top layer . . . 21
Figure 10. Bottom layer . . . 22
Figure 11. Schematic . . . 24
Figure 12. Characteristic waveforms (measured at 24 V input voltage and 280 W resistive load) . . . 26
Figure 13. Characteristic waveforms (measured at 28 V input voltage and 1000 W resistive load) . . . 26
Figure 14. MOSFET voltage (ch4) and current (ch3) without RC snubber . . . 27
Figure 15. MOSFET voltage (ch4) and current (ch3) with RC snubber . . . 27
Figure 16. Rectifier diode current (ch3) and voltage (ch4) without RDC snubber . . . 27
Figure 17. Rectifier diode current (ch3) and voltage (ch4) with RDC snubber . . . 27
Figure 18. Ch1, ch3 MOSFETs drain current, ch2, ch4 MOSFET drain-source voltage . . . 28
Figure 19. Startup, ch2, ch3 inverter voltage and current, ch4 DC bus voltage . . . 28
Figure 20. DC-DC converter efficiency with 20 V input . . . 28
Figure 21. DC-DC converter efficiency with 22 V input . . . 28
Figure 22. DC-DC converter efficiency with 24 V input . . . 28
Figure 23. DC-DC converter efficiency with 26 V input . . . 28
Figure 24. DC-DC converter efficiency with 28 V input . . . 29
Figure 25. Converter efficiency . . . 29
Figure 26. Technical specification for 1.5 mH 2.5 A inductor L4 (produced by MAGNETICA) . . . 35
Figure 27. Technical specification for 1 kW, 100 kHz switch mode power transformer TX1 (produced by MAGNETICA) . . . 36
Figure 28. Dimensional drawing . . . 37

1 System description

In a UPS system, as shown in *Figure 2*, a DC-AC converter is always used to convert the DC power from the batteries to AC power used to supply the load. The basic scheme also includes a battery pack, a battery charger which converts AC power from the grid into DC power, and a transfer switch to supply the load from the mains or from the energy storage elements if a line voltage drop or failure occurs.

Figure 2. Block diagram of an offline UPS system

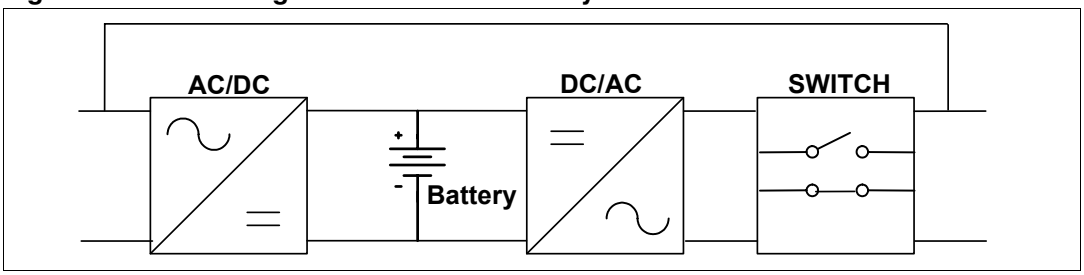

Another application where a DC-AC converter is always required is shown in the block diagram of *Figure 3*. In this case, the converter is part of a conversion scheme commonly used in standalone photovoltaic systems. An additional DC-DC converter operates as a battery charger while performing a maximum power point tracking algorithm (MPPT), which is necessary to maximize the energy yield from the PV array. The battery pack is always present to store energy when solar radiation is available and release it at night or during hours of low insolation.

Figure 3. Possible use of a DC-AC converter in standalone PV conversion

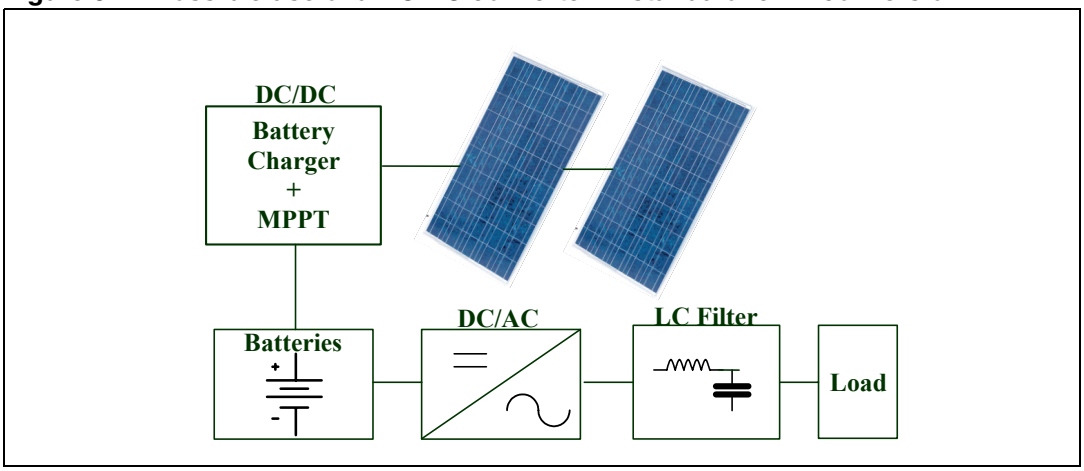

A possible implementation of an isolated DC-AC converter, which can be successfully used in both the above mentioned applications, is given in the block diagram of *Figure 4*. It consists of three main sections:

1. The DC-DC converter
2. The DC-AC converter
3. The power supply section

Figure 4. Block diagram of the proposed conversion scheme

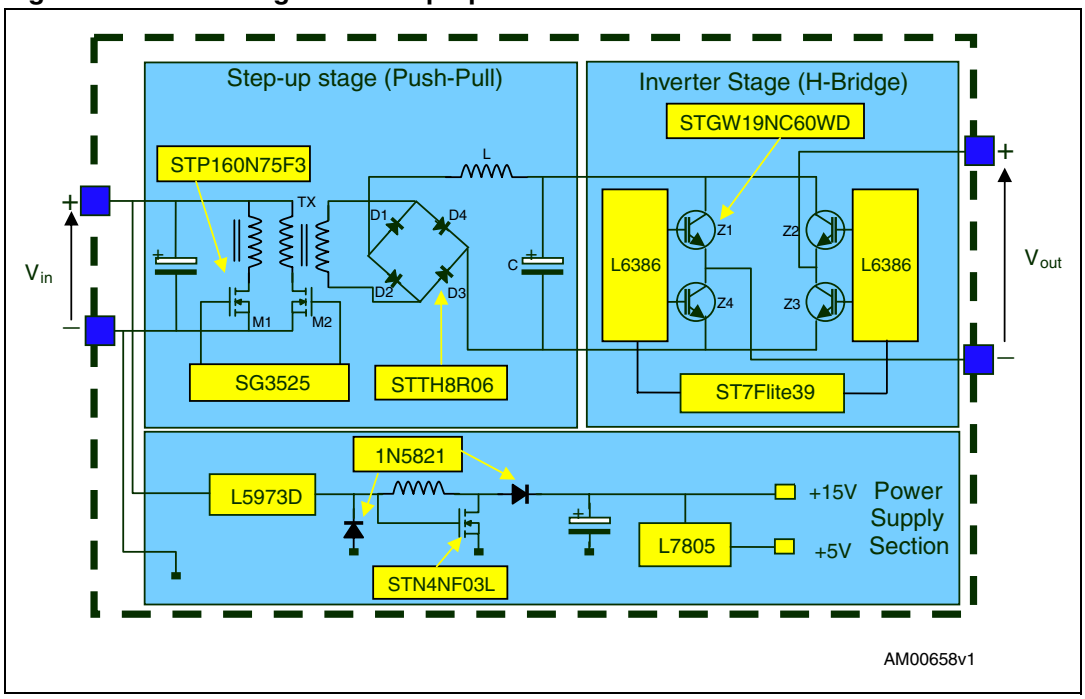

The DC-DC section is a critical part of the converter design. In fact, the need for high overall efficiency (close to 90% or higher) together with the specifications for continuous power rating, low input voltage range leading to high input current, and the need for high switching frequency to minimize weight and size of passive components, makes it a quite challenging design.

Due to the constraints given by the specifications given in *Table 1*, few topology solutions are suitable to meet the efficiency target. Actually, since the input voltage of the DC-AC converter must be at least equal to 350 V, it is not feasible to use non-isolated DC-DC converters. Moreover, the output power rating prevents the use of single switch topologies such as the flyback and the forward. Among the remaining isolated topologies, the half bridge and full bridge are more suitable for high DC input voltage applications and also characterized by the added complexity of gate drive circuitry of the high side switches.

Table 1. System specifications

Specification	Value
Nominal input voltage	24 V
Output voltage	230 Vrms, 50 Hz
Output power	1kW
Efficiency	90%
Switching frequency	100 kHz (DC-DC); 16 kHz (DC-AC)

Due to such considerations, the push-pull represents the most suitable choice. This topology features two transistors on the primary side and a center tapped high frequency transformer, as shown in the step-up section in *Figure 4*. It is quite efficient at low input voltage making it widely used in battery powered UPS applications. Both power devices are ground referenced with consequent simple gate drive circuits. They are alternatively turned

on and off in order to transfer power to each primary of the center tapped transformer. Contemporary conduction of both devices must be avoided by limiting the duty cycle value of the constant frequency PWM modulator to less than 0.5. The PWM modulator should also prevent unequal ON times for the driving signals since this would result in transformer saturation caused by the "Flux Walking" phenomenon.

The basic operation is similar to a forward converter. In fact, when a primary switch is active, the current flows through the rectifier diodes, charging the output inductor, while when both the switches are off, the output inductor discharges. It is important to point out that the operating frequency of the output inductor is twice the switching frequency.

A transformer reset circuit is not needed thanks to the bipolar flux operation, which also means better transformer core utilization with respect to single-ended topologies.

The main disadvantage of the push-pull converter is the breakdown voltage of primary power devices which has to be higher than twice the input voltage. In fact, when voltage is applied to one of the two transformer primary windings by the conduction of a transistor, the reflected voltage across the other primary winding puts the drain of the off state transistor at twice the input voltage with respect to ground. This is the reason why push-pull converters are not suitable for high input voltage applications.

For the above mentioned reasons, the voltage fed push-pull converter, shown in *Figure 4*, is chosen to boost the input voltage from 24 V to a regulated 350 V, suitable for optimal inverter operation. The high voltage conversion ratio can be achieved by proper transformer turns ratio design, taking into account that the input to output voltage transfer function is given by:

Equation 1

$$V_{out} = 2\frac{N_2}{N_1}DV_{in}$$

The duty cycle is set by a voltage mode PWM regulator (SG3525) to keep a constant output DC bus voltage. This voltage is then converted into AC using a standard H-bridge converter implemented with four ultrafast switching IGBTs in PowerMESH™ technology, switching at 16 kHz. The switching strategy, based on PWM sinusoidal modulation, is implemented on an 8-bit ST7lite39 microcontroller unit. This allows the use of a simple LC circuit to obtain a high quality sine wave in terms of harmonic content.

The power supply section consists of a buck-boost converter to produce a regulated 15 V from a minimum input voltage of 4 V. The circuit can be simply implemented by means of a L5973 device, characterized by an internal P-channel DMOS transistor and few external components. In this way, it is possible to supply all the driving circuits and the PWM modulator. A standard linear regulator, L7805, provides 5 V supply to the microcontroller unit.

2 Design considerations

The basic operation of a voltage fed push-pull converter is shown in *Figure 5*, where theoretical converter waveforms are highlighted. In practice, significant overvoltages across devices M1, M2 and across the four rectifier diodes are observed in most cases due to the leakage inductance of the high frequency transformer. As a consequence, the breakdown voltage of primary devices must be greater than twice the input voltage, and the use of snubbing and/or clamping circuits is often helpful.

Special attention has to be paid to transformer design, due to the difficulties in minimizing the leakage inductance and implementing low-voltage high-current terminations. Moreover, imbalance in the two primary inductance values must be avoided both by symmetrical windings and proper printed circuit board (PCB) layout. While transformer construction techniques guarantee good symmetry and low leakage inductance values, asymmetrical layout due to inappropriate component placement can be the source of different PCB trace inductances. Whatever the cause of a difference in peak current through the switching elements, transformer saturation in voltage mode push-pull converters can occur in a few switching cycles with catastrophic consequences.

Figure 5. Push-pull converter typical waveforms

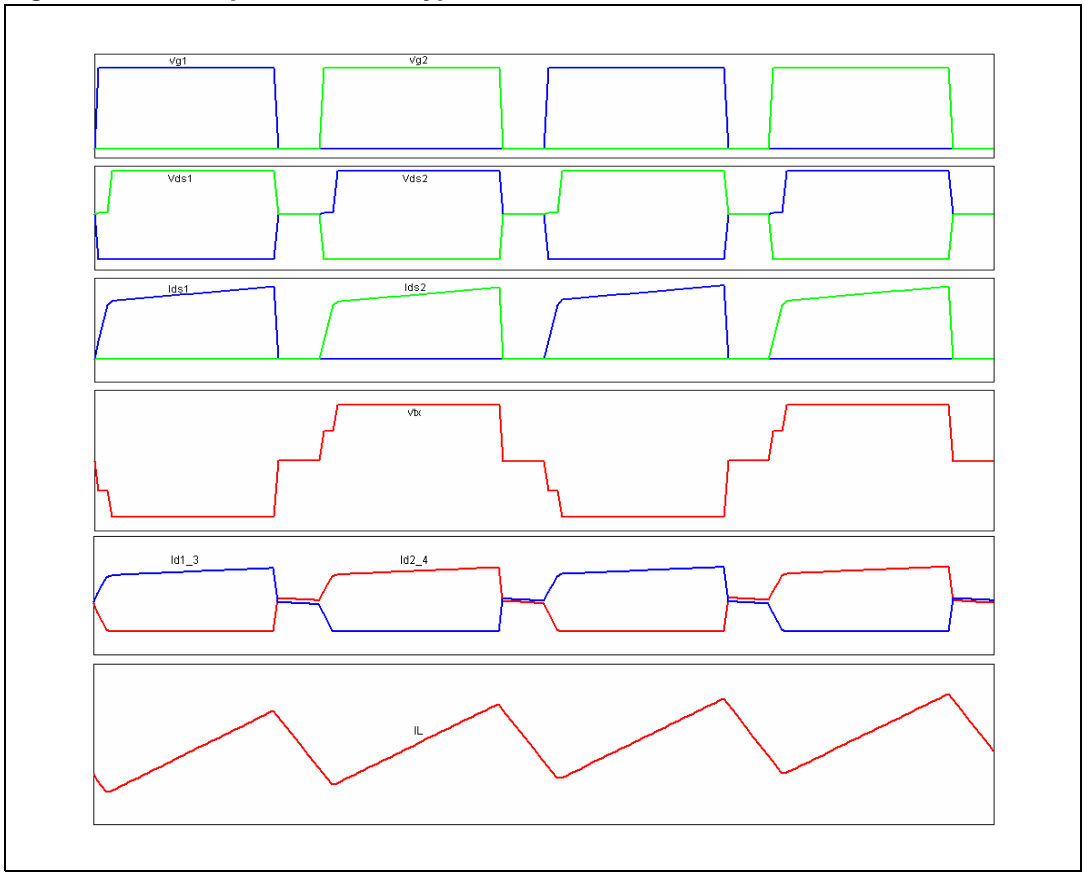

Starting from the specifications in *Table 2*, a step-by-step design procedure and some design hints to obtain a symmetrical layout are given below.

Table 2. Push-pull converter specifications

Specification	Symbol	Value
Nominal input voltage	V_{in}	24 V
Maximum input voltage	V_{inmax}	28 V
Minimum input voltage	V_{inmin}	20 V
Nominal output power	P_{out}	1000 W
Nominal output voltage	V_{out}	350 V
Target efficiency	η	> 90%
Switching frequency	f	100 kHz

A switching frequency of f = 100 kHz was chosen to minimize passive components size and weight, then the following step-by-step calculation was done:

- Switching period:

Equation 2

$$T = \frac{1}{f} = \frac{1}{10^5} = 10\ \mu s$$

- Maximum duty cycle

The theoretical maximum on time for each phase of the push-pull converter is:

Equation 3

$$t^*_{on} = 0.5T = 5\ \mu s$$

Since deadtime has to be provided in order to avoid simultaneous device conduction, it is better to choose the maximum duty cycle of each phase as:

Equation 4

$$D_{max} = 0.9\frac{t^*_{on}}{T} = 0.45$$

This means a total deadtime of 1µs at maximum duty cycle, occurring for minimum input voltage operation.

- Input power

Assuming 90% efficiency the input power is:

Equation 5

$$P_{in} = \frac{P_{out}}{0.9} = 1111W$$

- Maximum average input current:

Equation 6

$$I_{in} = \frac{P_{in}}{V_{in_{min}}} = \frac{1111}{20} = 55.55\,A$$

- Maximum equivalent flat topped input current:

Equation 7

$$I_{pft} = \frac{I_{in}}{2D_{max}} = \frac{55.55}{0.9} = 61.72\,A$$

- Maximum input RMS current:

Equation 8

$$I_{in_{RMS}} = I_{pft}\sqrt{2D_{max}} = 58.55A$$

- Maximum MOSFET RMS current:

Equation 9

$$I_{Mos_{RMS}} = I_{pft}\sqrt{D_{max}} = 41.4A$$

- Minimum MOSFET breakdown voltage:

Equation 10

$$V_{Brk_{Mos}} = 1.3 \bullet 2 \bullet V_{in_{Max}} = 72.8\,V$$

- Transformer turns ratio:

Equation 11

$$N = \frac{N_2}{N_1} = \frac{V_{out}}{2V_{in_{min}}D_{max}} = 19$$

- Minimum duty cycle value:

Equation 12

$$D_{min} = \frac{V_{out}}{2NV_{in_{max}}} = 0.32$$

- Duty cycle at nominal input voltage:

Equation 13

$$D_{min} = \frac{V_{out}}{2NV_{in}} = 0.38$$

- Maximum average output current:

Equation 14

$$I_{out} = \frac{P_{out}}{V_{out}} = 2.86\,A$$

- Secondary maximum RMS current

Assuming that the secondary top flat current value is equal to the average output value the rms secondary current is:

Equation 15

$$I_{sec_{RMS}} = I_{out}\sqrt{D_{max}} = 1.91\,A$$

- Rectifier diode voltage:

Equation 16

$$V_{diode} = NV_{in_{Max}} = 532\,V$$

- Output filter inductor value:

Equation 17

$$L_{min} \geq \left(\frac{N_2}{N_1}V_{in} - V_{out}\right)\frac{t_{on_{Max}}}{\Delta I}$$

Assuming a ripple current value ΔI= 15% I_{out} = 0.43A, the minimum value for the output filter inductance is:

Equation 18

$$L_{min} = 1.109\ mH$$

With this value of inductance continuous current mode (CCM) operation is guaranteed for a minimum output current of:

Equation 19

$$I_{out_{Min}} = \frac{\Delta I}{2} = 0.215\,A$$

which means a minimum load of 75 W is required for CCM operation. The chosen value for this design is L=1.5 mH.

- Output filter capacitor value:

Equation 20

$$C = \frac{1}{8}\frac{\Delta I_L}{\Delta V_0}T_s$$

Considering a maximum output ripple value equal to:

Equation 21

$$\Delta V_0 = 0.1\%V_{out} = 0.35\,V$$

the minimum value of capacitance is:

Equation 22

$$C_{min} = 1.53\ \mu F$$

and the equivalent series resistance (ESR) has to be lower than:

Equation 23

$$ESR_{max} = \frac{\Delta V_0}{\Delta I_L} = 0.81\ \Omega$$

- Input capacitor:

Equation 24

$$C_{in} = I_{Crms}\frac{\Delta T_{onMax}}{\Delta V_{in}}$$

where I_{crms} is the RMS capacitor current value given by:

Equation 25

$$I_{C_{rms}} = \sqrt{I_{In_{Rms}}^2 - I_{in}^2} = 19A$$

and

Equation 26

$$\Delta V_{in} = 0.1\% V_{in_{Max}} = 0.028V$$

then

Equation 27

$$C_{in} = I_{Crms}\frac{\Delta T_{onMax}}{\Delta V_{in}} = 3053\ \mu F$$

- HF transformer design

The design method is based on the K_g core geometry approach. The design can be done according to the specifications in *Table 3*.

Table 3. HF transformer design parameters

Specification	Symbol	Value
Nominal input voltage	V_{in}	24 V
Maximum input voltage	V_{inmax}	28 V
Minimum input voltage	V_{inmin}	20 V
RMS input current	I_{in}	41.4 A
Nominal output voltage	V_{out}	350 V
Output current	I_{out}	2.86 A
Switching frequency	f	100 kHz
Efficiency	η	98%
Regulation	α	0.05%
Max operating flux density	B_m	0.05T
Window utilization	K_u	0.3
Duty cycle	D_{max}	0.45
Temperature rise	T_r	30 °C

The first step is to compute the transformer apparent power given by:

Equation 28

$$P_t = \frac{P_0}{\eta} + P_0 = (\frac{1}{\eta} + 1)V_0 I_0 = 2021 \quad W$$

The second step is the electrical condition parameter calculation K_e:

Equation 29

$$K_e = 0.145 \bullet K_f^2 \bullet f^2 \bullet B_m^2 \left(10^{-4}\right)$$

where K_f=4 is the waveform coefficient (for square waves).

Equation 30

$$K_e = 0.145(4)^2(100.000)^2(0.05)^2\left(10^{-4}\right) = 5800$$

The next step is to calculate the core geometry parameter:

Equation 31

$$K_g = \frac{P_t}{2K_e\alpha} = 0.348 \text{ cm}^5$$

The K_g constant is related to the core geometrical parameters by the following equation:

Equation 32

$$K_g = \frac{W_a A_c^2 K_u}{MLT}$$

where W_a is the core window area, A_c is the core cross sectional area and MLT is the mean length per turn.

For example, choosing an E55/28/21 core with N27 ferrite, having

- W_a= 2.8 cm^2
- A_c= 3.5 cm^2
- MLT= 11.3 cm

the resulting K_g factor is:

- K_g= 0.91 cm^2

which is then suitable for this application.

Once the core has been chosen, it is possible to calculate the number of primary turns as follows:

Equation 33

$$N_1 = \frac{V_{in_{min}} D_{max} T}{\Delta B A_c} = 2 \text{ turns}$$

The primary inductance value is:

Equation 34

$$L_p = N^2 A_L = 4 \bullet 5800 \text{ nH} = 23.2 \text{ } \mu H$$

and the number of secondary turns is:

Equation 35

$$N_2 = N \bullet N1 = 38 \text{ turns}$$

At this point wires must be selected in order to implement primary and secondary windings. At 100 kHz the current penetration depth is:

Equation 36

$$\delta = \frac{6.62}{\sqrt{f}} = 0.0209 \text{ cm}$$

Then, the wire diameter can be selected as follows:

Equation 37

$$d = 2\delta = 0.0418 \text{cm}$$

and the conductor section is:

Equation 38

$$A_W = \pi \frac{d^2}{4} = 0.00137 cm^2$$

Checking the wire table we notice that AWG26, having a wire area of A_{WAWG26} = 0.00128 cm^2, can be used in this design. Considering a current density J = 500 A/cm^2 the number of primary wires is given by:

Equation 39

$$S_{np} = \frac{A_{wp}}{A_{w_{AWG26}}} = 62$$

where:

Equation 40

$$A_{wp} = \frac{I_{in}}{J} = 0.08\, cm^2$$

Since the AWG26 has a resistance of 1345 μΩ/cm, the primary resistance is:

Equation 41

$$r_p = \frac{1345 \mu\Omega / cm}{62} = 21.69 \mu\Omega / cm$$

and so the value of resistance for the primary winding is:

Equation 42

$$R_p = N_1 \bullet MLT \bullet r_p = 490.1\ \mu\Omega$$

Using the same procedure, the secondary winding is:

Equation 43

$$A_{ws} = \frac{I_{out}}{J} = 0.00572\ \ cm^2$$

Equation 44

$$S_{ns} = \frac{A_{ws}}{A_{w_{AWG26}}} = 5$$

Equation 45

$$r_s = \frac{1345 \mu\Omega / cm}{5} = 269 \mu\Omega / cm$$

Equation 46

$$R_s = N_2 \bullet MLT \bullet r_s = 115.5\, m\Omega$$

The total copper losses are:

Equation 47

$$P_{Cu} = P_p + P_s = R_p I^2_{in} + R_s I^2_s = 1.78W$$

And transformer regulation is:

Equation 48

$$\alpha = \frac{P_{cu}}{P_{out}} 100 = 0.178\%$$

From the core loss curve of N27 material, at 55 °C, 50mT and 100 kHz, the selected core has the following losses:

Equation 49

$$P_V = 28.1 \frac{kW}{m^3} \bullet V_e = 1.23\ W$$

Where V_e= 43900 mm^3 is the core volume. The transformer temperature rise is:

Equation 50

$$T_r = R_{th} \bullet (P_{Cu} + P_V) = 33\ ^oC$$

with

Equation 51

$$R_{th} = 11\ \frac{^oC}{W}$$

- Output inductor

The output filter inductor can be made using powder cores to minimize eddy current losses and introduce a distributed air gap into the core. The design parameters are shown in *Table 4*:

Table 4. Output inductor design parameters

Specification	Symbol	Value
Minimum inductance value	L_{min}	1.5 mH
DC current	I_0	2.86 A
AC current	ΔI	0.41 A
Output power	P_0	1000 W
Ripple frequency	f_r	200 kHz
Operating flux density	B_m	0.3 T
Core material		Kool µ
Window utilization	K_u	0.4
Temperature rise	T_r	25 °C

The peak current value across the inductor is:

Equation 52

$$I_{pk} = I_0 + \frac{\Delta I}{2} = 3.06A$$

To select a proper core we must compute the LI^2_{pk} value:

Equation 53

$$LI^2_{pk} = 10.3\,mH \bullet A$$

Knowing this parameter, from Magnetics' core chart, a 46.7 mm x 28.7 mm x 12.2 mm Kool μ toroid, with μ=60 permeability and A_L = 0.086 nH/turn can be selected. The required number of turns is then:

Equation 54

$$N = \sqrt{\frac{L}{A_L}} = 132 \text{ turns}$$

The resulting magnetizing force (DC bias) is:

Equation 55

$$H = 0.4\pi\frac{NI}{L_e} = 84.2 \text{ oersteds}$$

The initial value of turns has to be increased by dividing it by 0.8 (as shown in the data catalog) to take into account the reduction of initial permeability (μ_e = 39 at full load) at nominal current value. Then, the adjusted number of turns is:

Equation 56

$$N = 165 \text{ turns}$$

The wire table shows that at 3 A the AWG20 can be used. With this choice, the maximum number of turns per layer, for the selected core, is N_{layer}= 96 and the resistance per single layer is r_{layer}= 0.166Ω. The total winding resistance is then:

Equation 57

$$R = \frac{N}{N_{layer}} r_{layer} = 0.38\Omega$$

and the copper losses are:

Equation 58

$$P_{cu} = RI^2_o = 3.1 \text{ W}$$

The core losses can be evaluated as follows:

Equation 59

$$P_L = kB_{ac}^{2.12}f^{1.23} = 2.047mW/g$$

Equation 60

$$B_{ac} = \frac{0.4\pi N\frac{\Delta I}{2}\mu_e\left(10^{-4}\right)}{MPL} = 0.0137T$$

where MPL=11.8 cm is the magnetic path length. Since the core weight is 95.8 g, the core losses are:

Equation 61

$$P_L = 0.2\,W$$

- Analysis of the converter losses

Once the transformer has been designed, the next step in performing the loss analysis is to choose the power devices both for the input and output stage of the push-pull converter. According to the calculations given above the following components have been selected:

Table 5. Power MOSFET

Device	Type	$R_{DS(on)}$	t_r+t_f	V_{br}	I_d at 100 °C
STP160N75F3	Power MOSFET	4.5 mΩ	70 ns+15 ns	75 V	96 A

Table 6. Diode

Device	Type	V_F at 175 °C	t_{rrMax}	V_{RRM}	I_F at 100 °C
STTH8R06	Ultrafast diode	1.4 V	25 ns	600 V	8 A

MOSFET and diode losses can be separated into conduction and switching losses which can be estimated, in the worst case operating condition (junction temperature of 100 °C), with the following equations:

Equation 62

$$P_{cond} = 1.6R_{ds_{ON}}I^2_{Mos_{RMS}} = 12.5W$$

Equation 63

$$P_{gate} = Q_g V_{gs} f = 0.165W$$

Equation 64

$$P_{SW_{(ON+OFF)}} = \frac{1}{2}\frac{V_{Off}I_{mos}(t_r + t_f)}{T} = 8.5\,W$$

Equation 65

$$P_{cond_{Diode}} = V_F I_{sec_{RMS}} = 2.67W$$

Equation 66

$$P_{diode\ sw} = V_{RM} I_{RR} t_b f = 2.4\,W$$

Note: Assuming: $t_B = t_{rr}/2$, $V_{RM} = 350$ V

Converter losses are distributed according to the graphic in *Figure 6*, where PCB trace losses and control losses are not considered. What is important to note is that primary switch conduction accounts for 36% of total DC-DC converter losses. This contribution can be reduced by paralleling either two or three power devices. For example, by paralleling three STP160N75F3s, a reduction in MOSFET conduction losses of 33% is achieved. Thus MOSFET conduction losses account for 16% of total DC-DC converter losses, resulting in a 1.8% efficiency improvement.

Figure 6. Distribution of converter losses

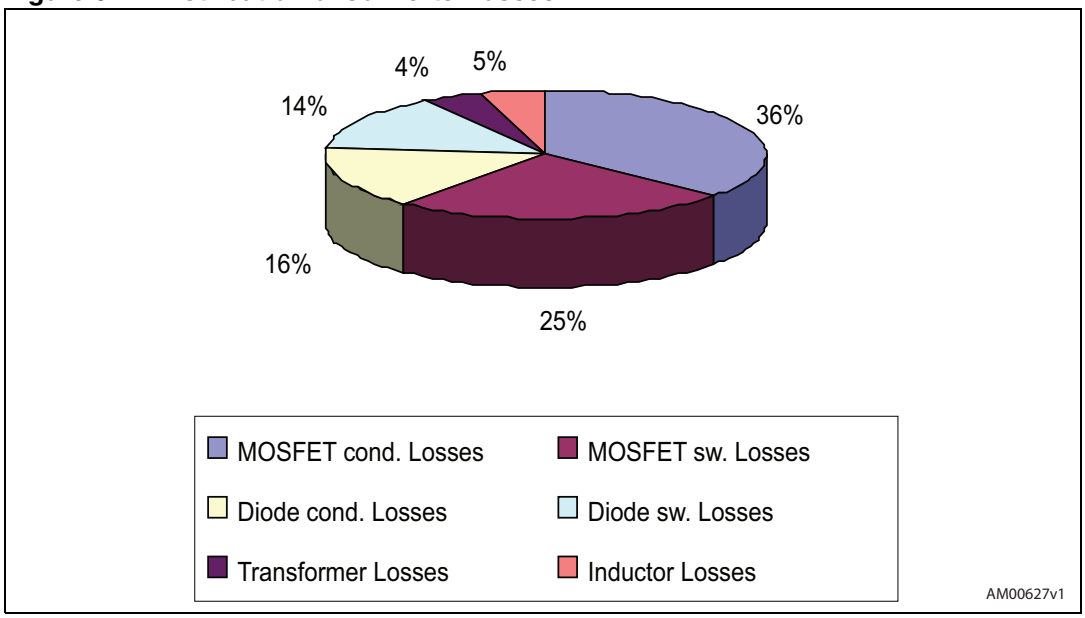

Figure 7. Distribution of losses with 3 STP160N75F3s paralleled

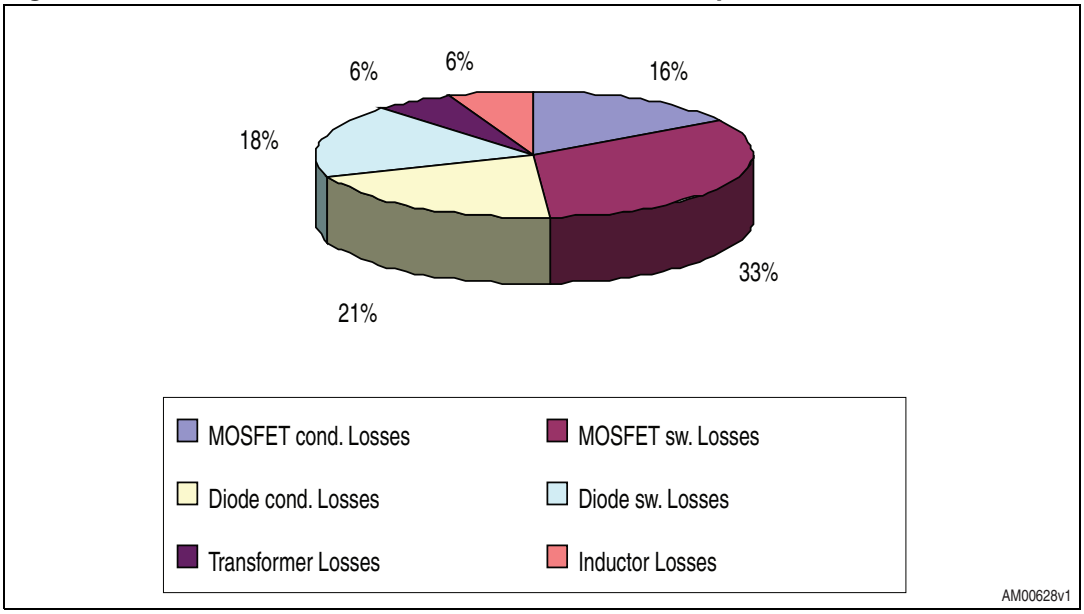

2.1 Layout considerations

Because of the high power level involved with this design, the parasitic elements must be reduced as much as possible. Proper operation of the push-pull converter can be assured through geometrical symmetry of the PCB board. In fact, geometrical symmetry leads to electrical symmetry, preventing a difference in the current values across the two primary windings of the transformer which can be the cause of core saturation. The output stage of the converter has also to be routed with a certain degree of symmetry even if in this case the impact of unwanted parasitic elements is lower because of lower current values with respect to the input stage. In *Figure 8*, *Figure 9* and *Figure 10*, a symmetrical layout designed for the application is shown.

Figure 8. Component placement

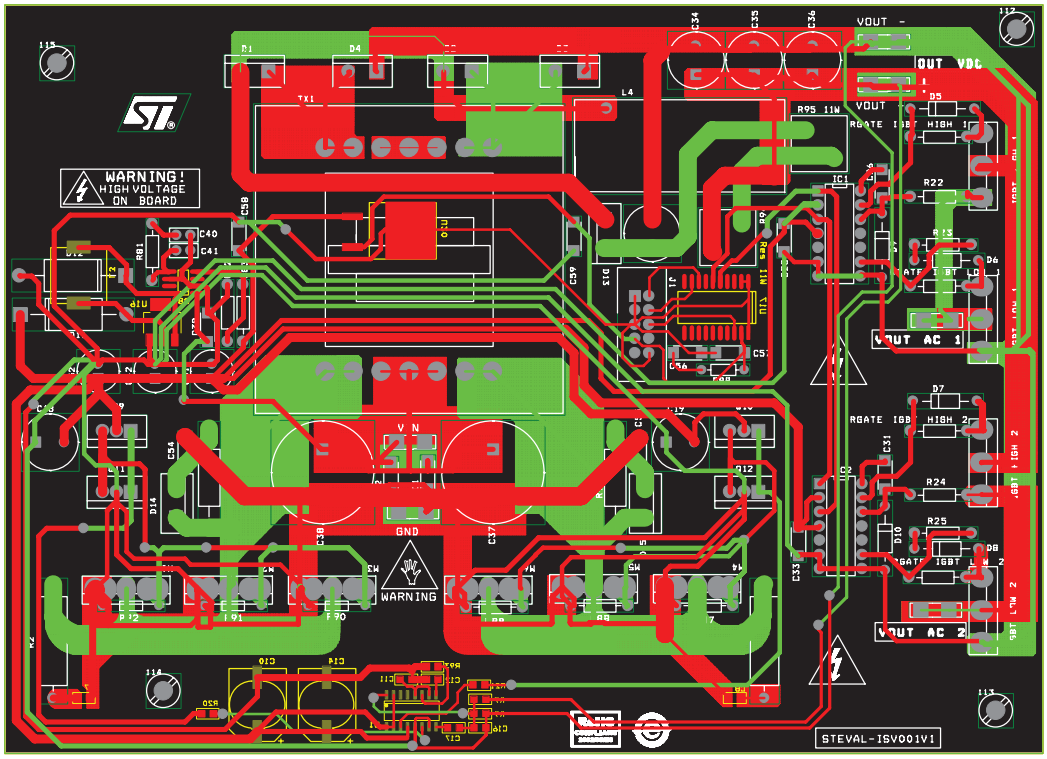

AM00629v1

Figure 9. Top layer

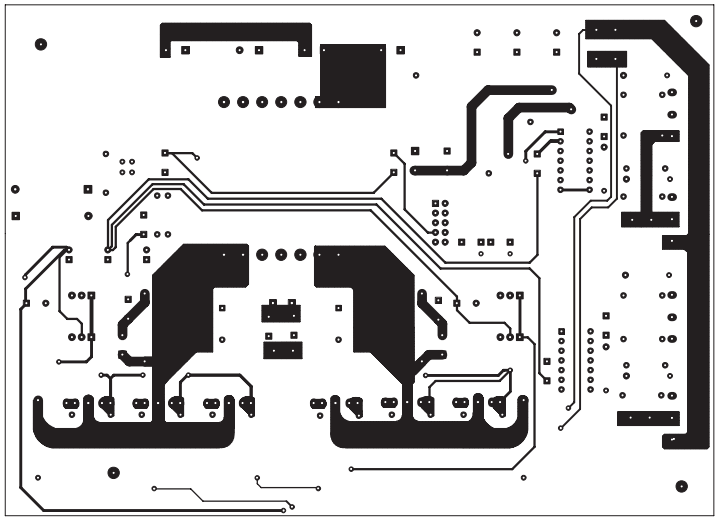

AM00630v1

Figure 10. Bottom layer

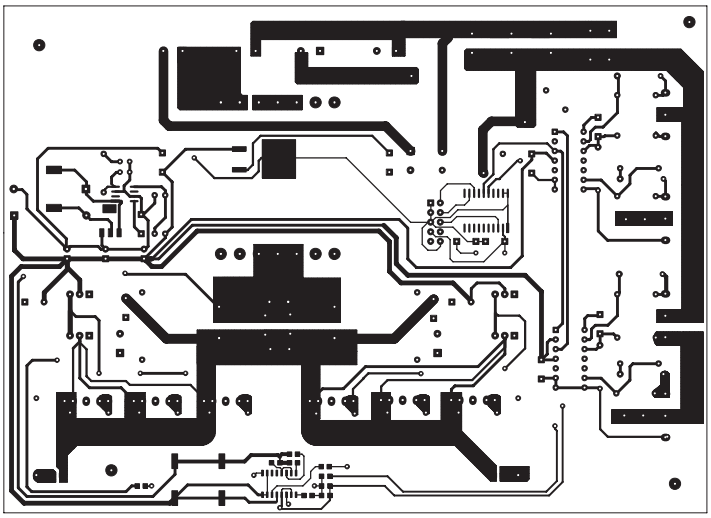

To obtain geometrical symmetry the HF transformer has been placed at the center of the board, which has been developed using double-sided, 140 μm FR-4 substrate with 135 x 185 mm size. In addition, this placement of the transformer is the most suitable since it is the bulkiest part of the board. Both the primary and secondary AC current loops are placed very close to the transformer in order to reduce their area and consequently their parasitic inductances. For this reason the MOSFET and rectifier diodes lie at the edges of the PCB. Input loop PCB traces show identical shapes to guarantee the same values of resistance and parasitic inductance. Also the IGBTs of the inverter stage lie at one edge of the board. This gives the advantage of using a single heat sink for each group of power components. The output filter is placed on the right side of the transformer, between the bridge rectifier and the inverter stage.

The power supply section lies on the left side of the transformer, simplifying the routing of the 15 V bus dedicated to supply all the control circuitry.

3 Schematic description

The schematic of the converter is shown in *Figure 11*. Three MOSFETs are paralleled in order to transfer power to each primary winding of the transformer. Both RC and RCD networks can be connected between the drain and source of the MOSFETs to reduce the overvoltages and voltage ringing caused by unclamped leakage inductance. The output of the transformer is rectified by a full bridge of ultrafast soft-recovery diodes. An RCD network is connected across the rectifier output to clamp the diode voltage to its steady state value and recover the reverse recovery energy stored in the leakage inductance. This energy is first transferred to the clamp capacitor and then partially diverted to the output through a resistor.

The IGBT full bridge is connected to the output of the push-pull stage. Their control signals are generated by an SG3525 voltage mode PWM modulator. Its internal clock, necessary to generate the 100 kHz modulation, is set by an external RC network. The PWM output stage is capable of sourcing or sinking up to 100 mA which can be enough to directly drive the gate of the MOSFETs devices. The PWM controller power dissipation, given by the sum of its own power consumption and the power needed to drive six STP160N75F3s at 100 kHz, can be evaluated with the following equation:

Equation 67

$$P_{Contoller\ tot} = 6Q_g f V_{drive} + V_s I_s = 1.3W$$

where V_s and I_s are the supply voltage and current.

Since this power dissipation would result in a high operating temperature of the IC, a totem pole driving circuit has been used to handle the power losses and peak currents, achieving a more favorable operating condition. This circuit was implemented by means of an NPN-PNP complementary pair of BJT transistors. The control and driver stage schematic is shown in *Figure 11*.

Figure 11. Schematic

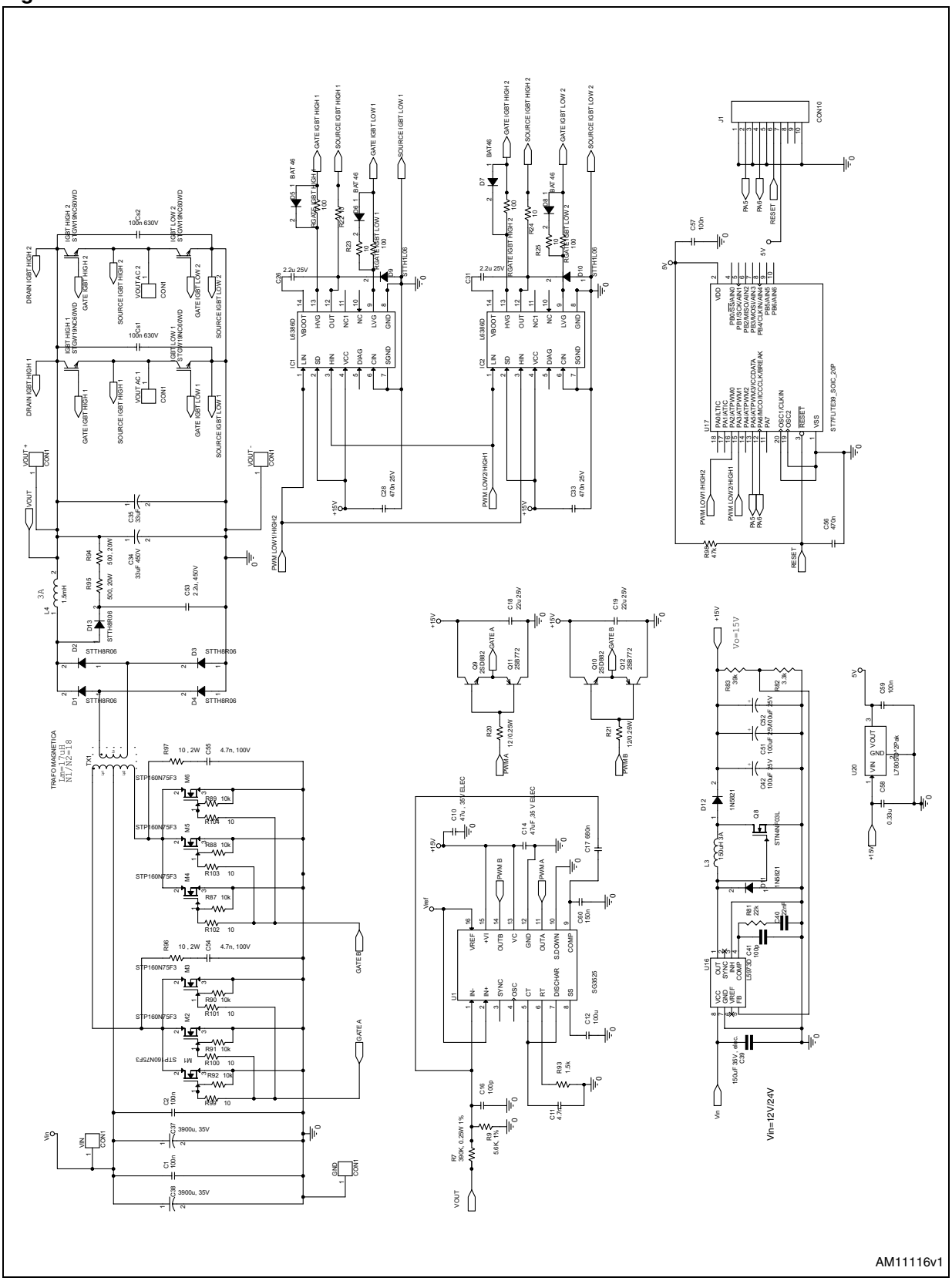

The PWM modulation of the H-bridge inverter is implemented on an ST7lite39 microcontroller connected to the gate drive circuit composed of two L6386, as shown in the schematic in *Figure 11*.

The auxiliary power supply section consists of an L5973D and an L7805, used to implement a buck-boost converter to decrease the battery voltage from 24 V to 15 V and from 15 V to 5 V respectively.

4 Experimental results

Typical voltage and current waveforms of the DC-AC converter and the efficiency curves of the push-pull DC-DC stage, measured at different input voltages, are shown below. In particular, *Figure 12* and *Figure 13* show both input and output characteristic waveforms of the DC-DC converter both in light load and full load condition.

The HF transformer leakage inductance, which is about 1% of the magnetizing inductance, is the cause of severe ringing across the input and the output power devices. MOSFETs voltage and current waveforms with and without the connection of a snubber network are shown in *Figure 14* and *15*, while *Figure 16* and *17* show the effect of the RCD clamp circuit connected across the rectifier bridge output. In *Figure 18* the current and the voltage across one of the three parallel-connected MOSFETs, powering each of the two windings of the transformer are shown, while in *Figure 19* it is possible to observe the variation of the inverter output voltage and current together with the DC-DC converter bus voltage. In *Figure 20*, *21*, *22*, *23* and *24*, the efficiency curves of the push-pull converter measured with an RL load are given. A maximum efficiency above 93% has been measured at nominal input voltage and 640 W output power. The minimum value of efficiency has been tested under low load and maximum input voltage. In *Figure 25*, the efficiency of the whole board is shown. The efficiency tests have been carried out connecting an RL load at the inverter output connectors, with 3 mH output inductor.

Figure 12. Characteristic waveforms (measured at 24 V input voltage and 280 W resistive load)

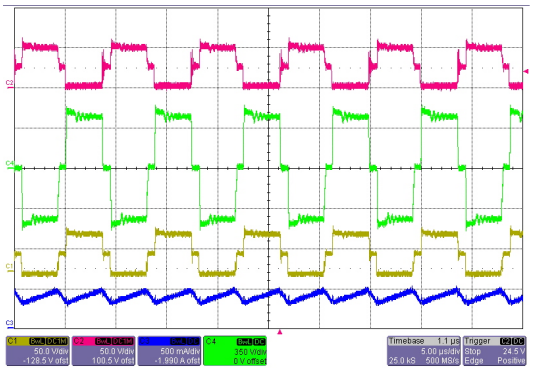

Ch1 and Ch2: MOSFETs drain source voltage; Ch4: HF transformer output voltage; Ch3: filter inductor current

Figure 13. Characteristic waveforms (measured at 28 V input voltage and 1000 W resistive load)

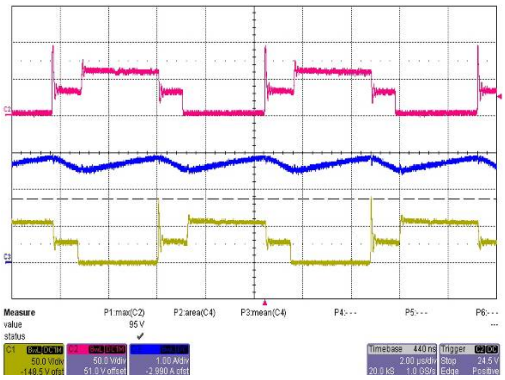

Ch1 and Ch2: MOSFETs drain source voltage; Ch3: filter inductor current

Figure 14. MOSFET voltage (ch4) and current (ch3) without RC snubber

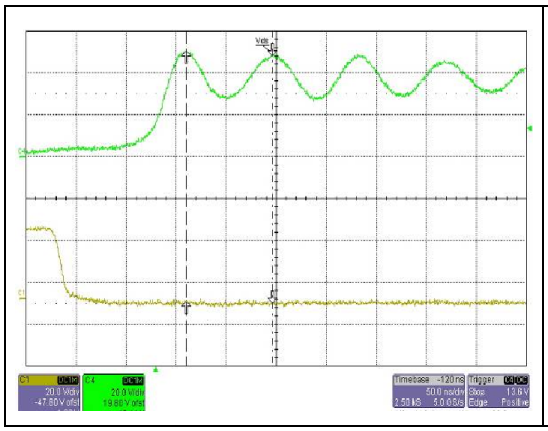

Figure 15. MOSFET voltage (ch4) and current (ch3) with RC snubber

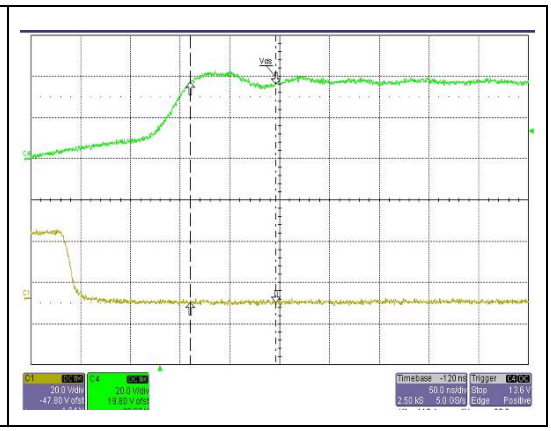

Figure 16. Rectifier diode current (ch3) and voltage (ch4) without RDC snubber

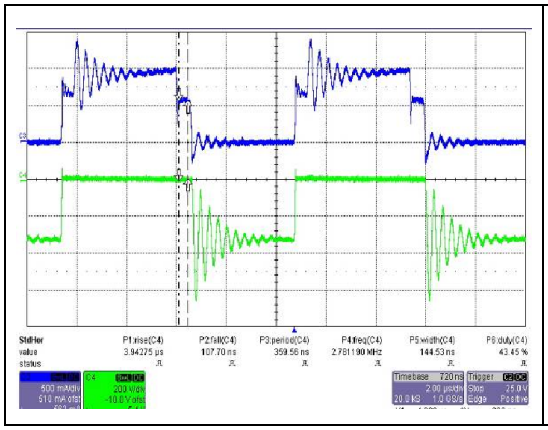

Figure 17. Rectifier diode current (ch3) and voltage (ch4) with RDC snubber

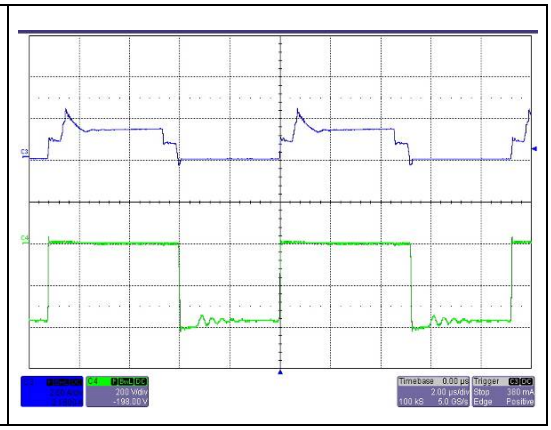

Figure 18. Ch1, ch3 MOSFETs drain current, ch2, ch4 MOSFET drain-source voltage

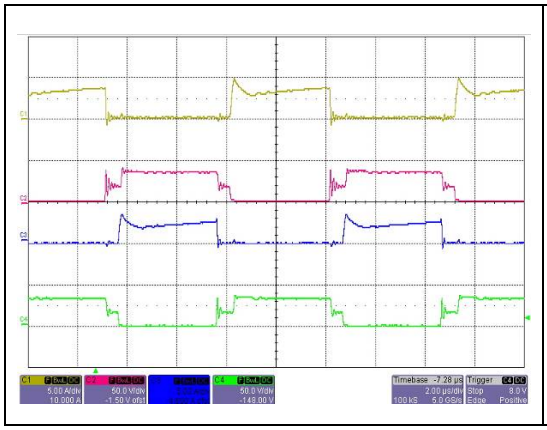

Figure 19. Startup, ch2, ch3 inverter voltage and current, ch4 DC bus voltage

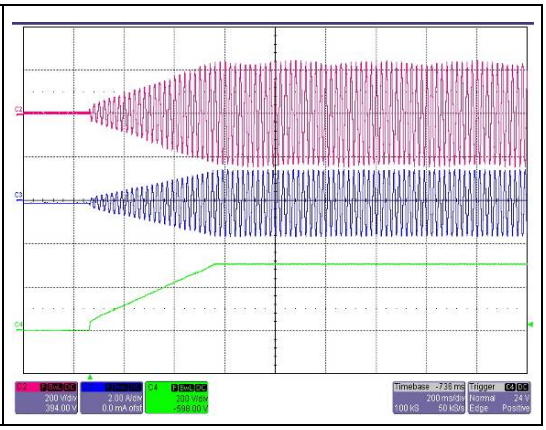

Figure 20. DC-DC converter efficiency with 20 V input

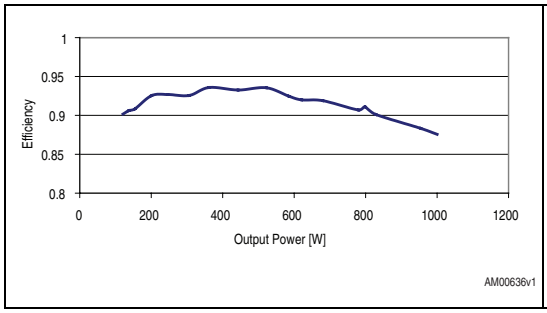

Figure 21. DC-DC converter efficiency with 22 V input

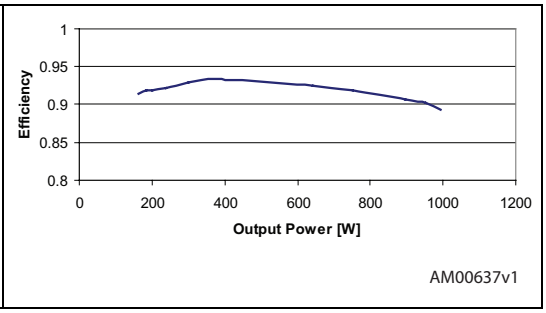

Figure 22. DC-DC converter efficiency with 24 V input

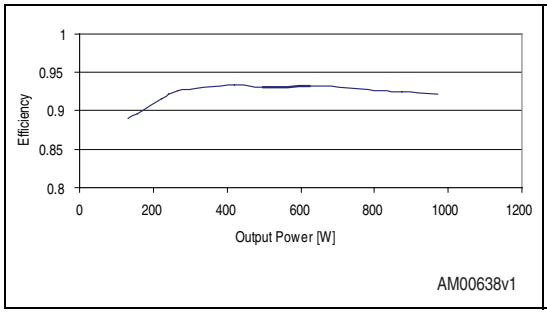

Figure 23. DC-DC converter efficiency with 26 V input

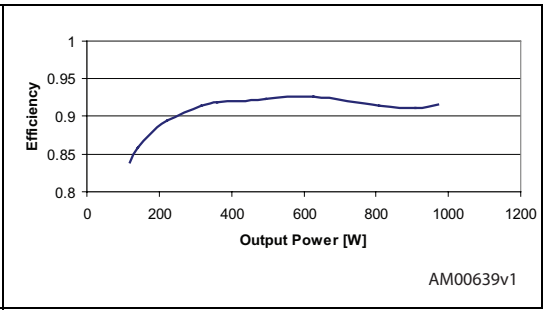

Figure 24. DC-DC converter efficiency with 28 V input

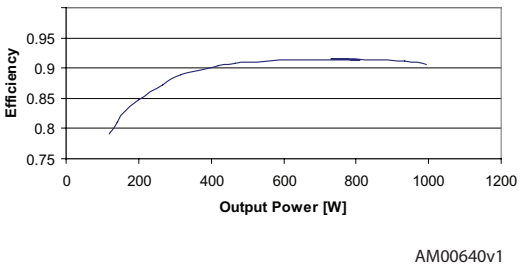

Figure 25. Converter efficiency

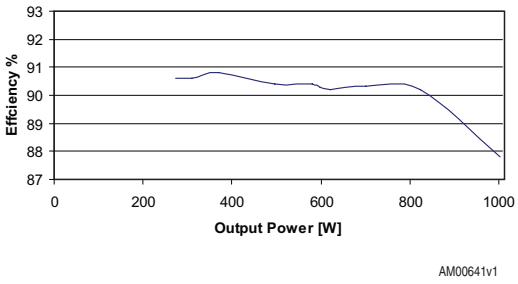

5 Conclusion

The theoretical analysis, design and implementation of a DC-AC converter, consisting of a push-pull DC-DC stage and a full-bridge inverter circuit, have been evaluated. Due to the use of the parallel connection of three STP160N75F3 MOSFETs the converter shows good performance in terms of efficiency. Moreover the use of an ST7lite39 8-bit microcontroller allows achieving simple control of the IGBTs used to implement the DC-AC stage. Any additional feature, such as regulation of the AC output voltage or protection requirements, can simply be achieved with firmware development.

6 Bibliography

1. Power Electronics: Converters, Applications and Design
2. Transformer and Inductor Design Handbook, Second Edition
3. Magnetic Core Selection for Transformers and Inductors, Second Edition
4. Switching Power Supply Design. New York.

Appendix A Component list

Table 7. Bill of material (BOM)

Component	Part value	Description	Supplier
Cs1	100 nF, 630 V	Polip. cap., MKP series	EPCOS
Cs2	100 nF, 630 V	Polip. cap., MKP series	EPCOS
C1	100 nF, 50 V	X7R ceramic cap.., B37987 series	EPCOS
C2	100 nF, 50 V	X7R ceramic cap., B37987 series	EPCOS
C57	100 nF, 50 V	X7R ceramic cap., B37987 series	EPCOS
C59	100 nF, 50 V	X7R ceramic cap., B37987 series	EPCOS
C10	47 µF, 35 V	SMD tantalum capacitor TAJ series	AVX
C11	4.7 nF, 25 V	SMD multilayer ceramic capacitor	muRata
C12	100 µF, 25 V	SMD X7R ceramic cap. C3225 series; size 1210	TDK
C14	47 µF, 35 V	SMD tantalum capacitor TAJ series	AVX
C16	100 pF, 25 V	SMD multilayer ceramic capacitor	muRata
C41	100 pF, 50 V	General purpose ceramic cap., radial	AVX
C17	680 nF, 25 V	SMD multilayer ceramic capacitor	muRata
C18	22 µF, 25 V	Electrolytic cap FC series	Panasonic
C19	22 µF, 25 V	Electrolytic cap. FC series	Panasonic
C26	2.2 µF, 25 V	X7R ceramic cap., B37984 series	EPCOS
C31	2.2 µF, 25 V	X7R ceramic cap., B37984 series	EPCOS
C28	470 nF, 25 V	X7R ceramic cap., B37984 series	EPCOS
C33	470 nF, 25 V	X7R ceramic cap., B37984 series	EPCOS
C34	33 µF, 450 V	Electrolytic cap. B43821 series	EPCOS
C35	33 µF, 450 V	Electrolytic cap. B43821 series	EPCOS
C37	3900 µF, 35 V	Elec. capacitor 0.012 Ω, YXH series	Rubycon
C38	3900 µF, 35 V	Elec. capacitor 0.012 Ω, YXH series	Rubycon
C39	150 µF, 35 V	Electrolytic cap. fc series	Panasonic
C40	22 nF, 50 V	General purpose ceramic cap., radial	AVX
C42	100 µF, 25 V	Electrolytic cap. fc series	Panasonic
C51	100 µF, 25 V	Electrolytic cap.fc series	Panasonic
C52	100 µF, 25 V	Electrolytic cap.fc series	Panasonic
C53	2.2 µF, 450 V	Elcrolytic capactor B43851 series	EPCOS
C54	4.7 nF, 100 V	Polip. cap., MKT series	EPCOS
C55	4.7 nF, 100 V	Polip. cap., MKT series	EPCOS
C56	470 nF, 50 V	X7R ceramic cap., B37984 series	EPCOS

Table 7. Bill of material (BOM) (continued)

Component	Part value	Description	Supplier
C58	0.33 µF, 50 V	X7R ceramic cap., B37984 series	EPCOS
C60	150 nF, 50 V	SMD multilayer ceramic capacitor	muRata
D1	STTH8R06D	Ultrafast high voltage rectifier; TO-220AC	STMicroelectronics
D2	STTH8R06 D	Ultrafast high voltage rectifier; TO-220AC	STMicroelectronics
D3	STTH8R06 D	Ultrafast high voltage rectifier; TO-220AC	STMicroelectronics
D4	STTH8R06 D	Ultrafast high voltage rectifier; TO-220AC	STMicroelectronics
D13	STTH8R06 D	Ultrafast high voltage rectifier; TO-220AC	STMicroelectronics
D5	BAT46	Small signal Schottky diode; SOD-123	STMicroelectronics
D6	BAT46	Small signal Schottky diode; SOD-123	STMicroelectronics
D8	BAT46	Small signal Schottky diode; SOD-123	STMicroelectronics
D7	BAT46	Small signal Schottky diode; SOD-123	STMicroelectronics
D9	STTH1L06	Ultrafast high voltage rectifier; DO-41	STMicroelectronics
D10	STTH1L06	Ultrafast high voltage rectifier; DO-41	STMicroelectronics
D11	1N5821	Schottky rectifier; DO-221AD	STMicroelectronics
D12	1N5821	Schottky rectifier; DO-221AD	STMicroelectronics
VOUT AC 1	CON1	FASTON	RS components
VOUT AC 2	CON1	FASTON	RS components
VOUT -	CON1	FASTON	RS components
VOUT +	CON1	FASTON	RS components
VIN	CON1	FASTON	RS components
GND	CON1	FASTON	RS components
IC1	L6386D	High-voltage high and low side driver; dip-14	STMicroelectronics
IC2	L6386D	High-voltage high and low side driver; dip-14	STMicroelectronics
IGBT LOW 1	STGW19NC60WD	N-channel 19 A - 600 V TO-247 PowerMESH™ IGBT	STMicroelectronics
IGBT HIGH 1	STGW19NC60WD	N-channel 19 A - 600 V TO-247 PowerMESH™ IGBT	STMicroelectronics
IGBT LOW 2	STGW19NC60WD	N-channel 19 A - 600 V TO-247 PowerMESH™ IGBT	STMicroelectronics
IGBT HIGH 2	STGW19NC60WD	N-channel 19 A - 600 V TO-247 PowerMESH™ IGBT	STMicroelectronics
J1	CON10	10-way idc connector commercial box header series	Tyco Electronics
L3	150 µH, 3 A	Power use SMD inductor; SLF12575T series	TDK
L4(1)	1174.0018 ST04	1.5 mH, filter inductor	MAGNETICA
M1	STP160N75F3	N-channel 75 V - 3.5 mΩ 120 A TO-220 STripFET™ Power MOSFET	STMicroelectronics
M2	STP160N75F3	N-channel 75 V - 3.5 mΩ 120 A TO-220 STripFET™ Power MOSFET	STMicroelectronics
M3	STP160N75F3	N-channel 75 V - 3.5 mΩ 120 A TO-220 STripFET™ Power MOSFET	STMicroelectronics

Table 7. Bill of material (BOM) (continued)

Component	Part value	Description	Supplier
M4	STP160N75F3	N-channel 75 V - 3.5 mΩ 120 A TO-220 STripFET™ Power MOSFET	STMicroelectronics
M5	STP160N75F3	N-channel 75 V - 3.5 mΩ 120 A TO-220 STripFET™ Power MOSFET	STMicroelectronics
M6	STP160N75F3	N-channel 75 V - 3.5 mΩ 120 A TO-220 STripFET™ Power MOSFET	STMicroelectronics
Q8	STN4NF03L	N-channel 30 V , 6.5 A SOT-223 STripFET™ II Power MOSFET	STMicroelectronics
Q9	2SD882	NPN Power BJT 30 V, 3 A transistor- SOT-32	STMicroelectronics
Q10	2SD882	NPN Power BJT 30 V, 3 A transistor- SOT-32	STMicroelectronics
Q11	2SB772	NPN Power BJT 30 V, 3 A transistor - SOT-32	STMicroelectronics
Q12	2SB772	NPN Power BJT 30 V, 3 A transistor - SOT-32	STMicroelectronics
RGATE IGBT LOW 1	100	SMD standard film res - 1/8 W - 1% - 100 ppm/°C	BC components
RGATE IGBT HIGH 1	100	SMD standard film res - 1/8 W - 1% - 100 ppm/°C	BC components
RGATE IGBT LOW 2	100	SMD standard film res - 1/8 W - 1% - 100 ppm/°C	BC components
RGATE IGBT HIGH 2	100	SMD standard film res - 1/8 W - 1% - 100 ppm/°C	BC components
R7	390 kΩ	SMD standard film res - 1/8 W - 1% - 100 ppm/°C	BC components
R9	5.6 kΩ	SMD standard film res - 1/8 W - 1% - 100 ppm/°C	BC components
R20	12 Ω	SMD standard film res - 1/8 W - 1% - 100 ppm/°C	BC components
R21			
R22	10 Ω	SMD standard film res - 1/8 W - 1% - 100 ppm/°C	BC components
R23			
R24			
R25			
R99			
R100			
R101			
R102			
R103			
R104			
R81	22 kΩ	Standard film res - 1/4 W 5%, axial 05	T-Ohm
R82	3.3 kΩ	Standard film res - 1/4 W 5%, axial 05	T-Ohm
R83	39 kΩ	Standard film res - 1/4 W 5%, axial 05	T-Ohm
R87	10 kΩ	SMD standard film res - 1/8 W - 1% - 100ppm/°C	BC components

Table 7. Bill of material (BOM) (continued)

Component	Part value	Description	Supplier
R88	10 kΩ	SMD standard film res - 1/8 W - 1% - 100ppm/°C	BC components
R89			
R90			
R91			
R92			
R93	1.5 kΩ	SMD standard film res - 1/8 W – 1% - 100ppm/°C	BC components
R94	470 Ω	High voltage 17 W ceramic resistor sbcv type	Meggit CGS
R95	470 Ω	High voltage 17 W ceramic resistor sbcv type	Meggit CGS
R96	10 Ω	Standard film res – 2 W 5%, axial 05	T-Ohm
R97			
R98	47 kΩ	Standard film res - 1/4 W 5%, axial 05	T-Ohm
TX1(2)	1356.0004 rev.01	Power transformer	MAGNETICA
U1	SG3525	Pulse width modulator SO-16 (narrow)	STMicroelectronics
U16	L5973D	2.5 A switch step down regulator; HSOP8	STMicroelectronics
U17	ST7FLITE39F2	8-bit microcontroller; SO-20	STMicroelectronics
U20	L7805	Positive voltage regulator; D^2PAK	STMicroelectronics
124	HEAT SINK	Part n. 78185, S562 cooled package TO-220; thermal res. 7.52 °C/W at length 70 mm width 40 mm height 57 mm	Aavid Thermalloy
125	HEAT SINK	Part n. 78350, SA36 cooled package TO-220; thermal res. 1.2°C/W at length 135 mm width 49.5 mm height 85.5 mm	Aavid Thermalloy
126			

1. The technical specification for this component is provided in *Figure 26*.
2. The technical specification for this component is provided in *Figure 27*.

Appendix B Product technical specification

Figure 26. Technical specification for 1.5 mH 2.5 A inductor L4 (produced by MAGNETICA)

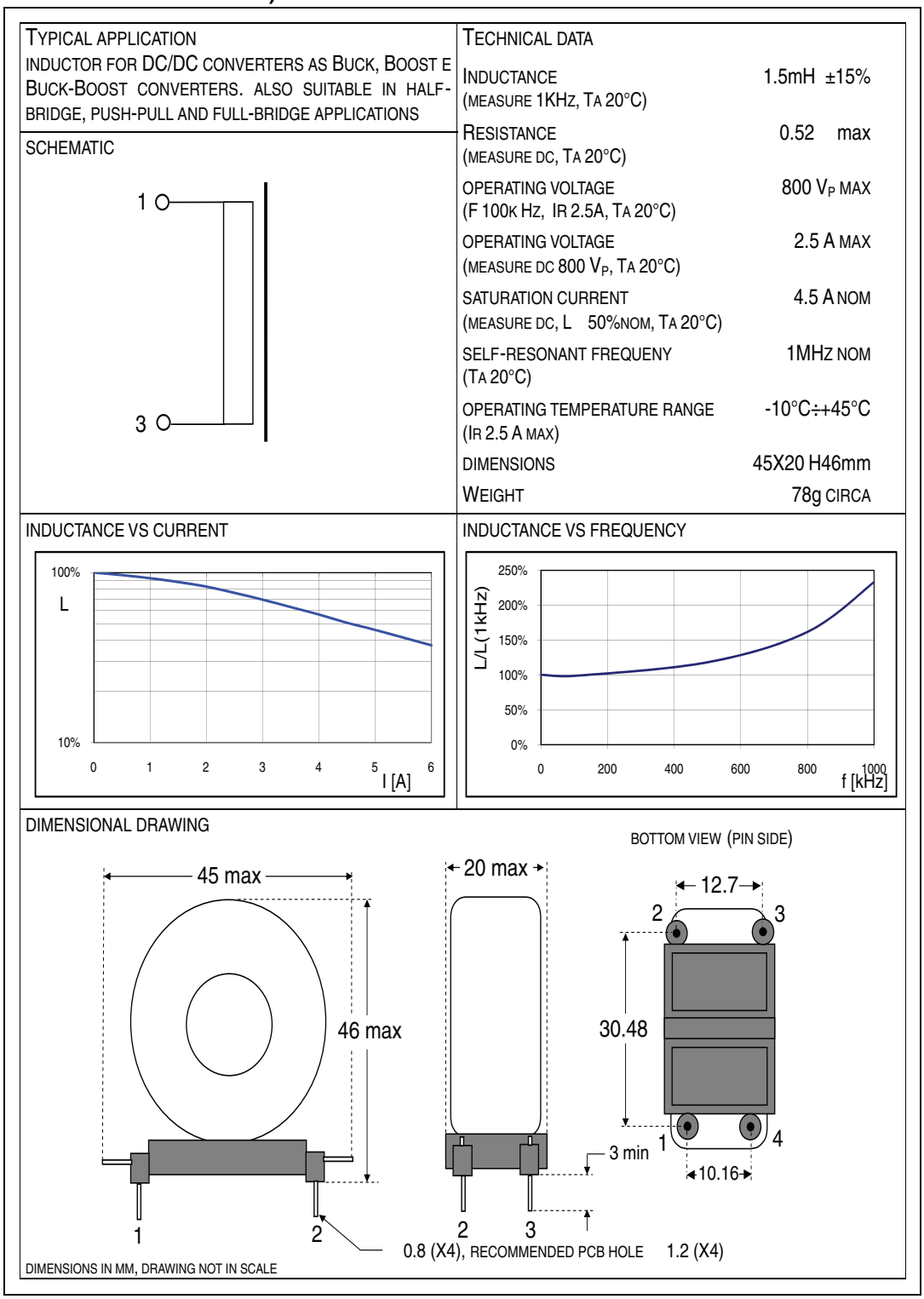

Figure 27. Technical specification for 1 kW, 100 kHz switch mode power transformer TX1 (produced by MAGNETICA)

TYPICAL APPLICATION

TRANSFORMER TO POWER APPLICATIONS WITH HALF - BRIDGE , PUSH -PULL E FULL -BRIDGE TYPOLOGY .

SCHEMATIC

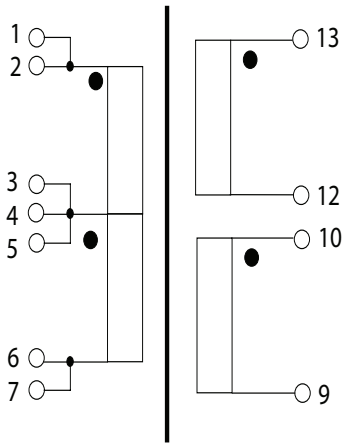

PRODUCT PICTURE

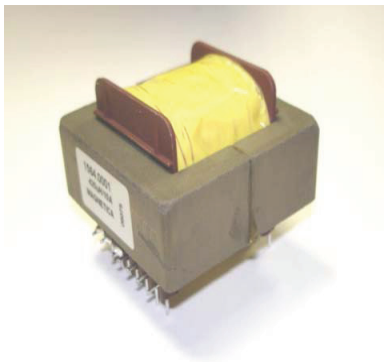

TECHNICAL DATA

INDUCTANCE
(MEASURE 1KHZ, TA 20°C)

PIN 1,2 – 3,4,5	17.2 uH MIN
PIN 3,4,5 – 6,7	17.2 uH MIN
PIN 9 – 13 (10-12 IN CC)	5.7 mH MIN

RESISTANCE
(MEASURE D .C, TA 20°C)

PIN 1,2 – 3,4,5	6 mΩ MAX
PIN 3,4,5 – 6,7	6 mΩ MAX
PIN 9 – 13 (10-12 IN CC)	90 mΩ MAX

TRANSFORMER RATIO
(MEASURE 10KHZ, 10-12 IN CC , TA 20°C)

PIN 13 – 9 ⇔ 1,2 – 3,4,5	18 ±5%
PIN 13 – 9 ⇔ 3,4,5 – 6,7	18 ±5%

LEAKAGE INDUCTANCE 0.11 % NOM
(MEASURE 9-13, 1-2-3-4-5-6-7 AND 10-12 IN C .C, F 10KHZ, TA 20°C)

OPERATING VOLTAGE 800 V_P MAX
(MEASURE 13-9, 10-12 IN CC , F 100KHZ , DUTY CYCLE 0.8,T A 20°C)

OPERATING CURRENT 2.5 A MAX
(MEASURE 13-9 WITH 1-2-3-4-5-6-7 IN CC ,
P_{MAX} 1KW ,F 100 KHZ, TA 20°C)

OPERATING FREQUENCY 100 KHZ NOM
(P_{MAX} 1KW , TA 20°C)

OPERATING TEMPERATURE RANGE -10°C ÷+45°C
(P_{MAX} 1KW, F 100KHZ)

INSULATION CLASS I
(P_{MAX} 1KW, TA 20°C)

PRIMARY TO SECONDARY INSULATION 2500V
(F 50HZ,DURATION TEST 2", TA 20°C)

MAXIMUM DIMENSIONS 57X57H45 mm

WEIGHT 292g CIRCA

PIN DESCRIPTION

PIN (*)	FUNCTION	PIN (*)	FUNCTION
1A	PRIMARY DRAIN A	8	NOT USED
2A	PRIMARY DRAIN A	9	SECONDARY GROUND
3B	PRIMARY +VB 24V	10D	INTERMEDIARY SECONDARY ACCESS
4B		11	MISSING , REFERENCE TO PCB ASSEMBLING
5B		12D	INTERMEDIARY SECONDARY ACCESS
6C	PRIMARY DRAIN B	13	SECONDARY 400V 2.5A
7C	PRIMARY DRAIN B	14	NOT USED

(*)PIN WITH THE SAME SUBSCRIPT MU ST BE CONNECTED TOGETHER ON PCB

Figure 28. Dimensional drawing

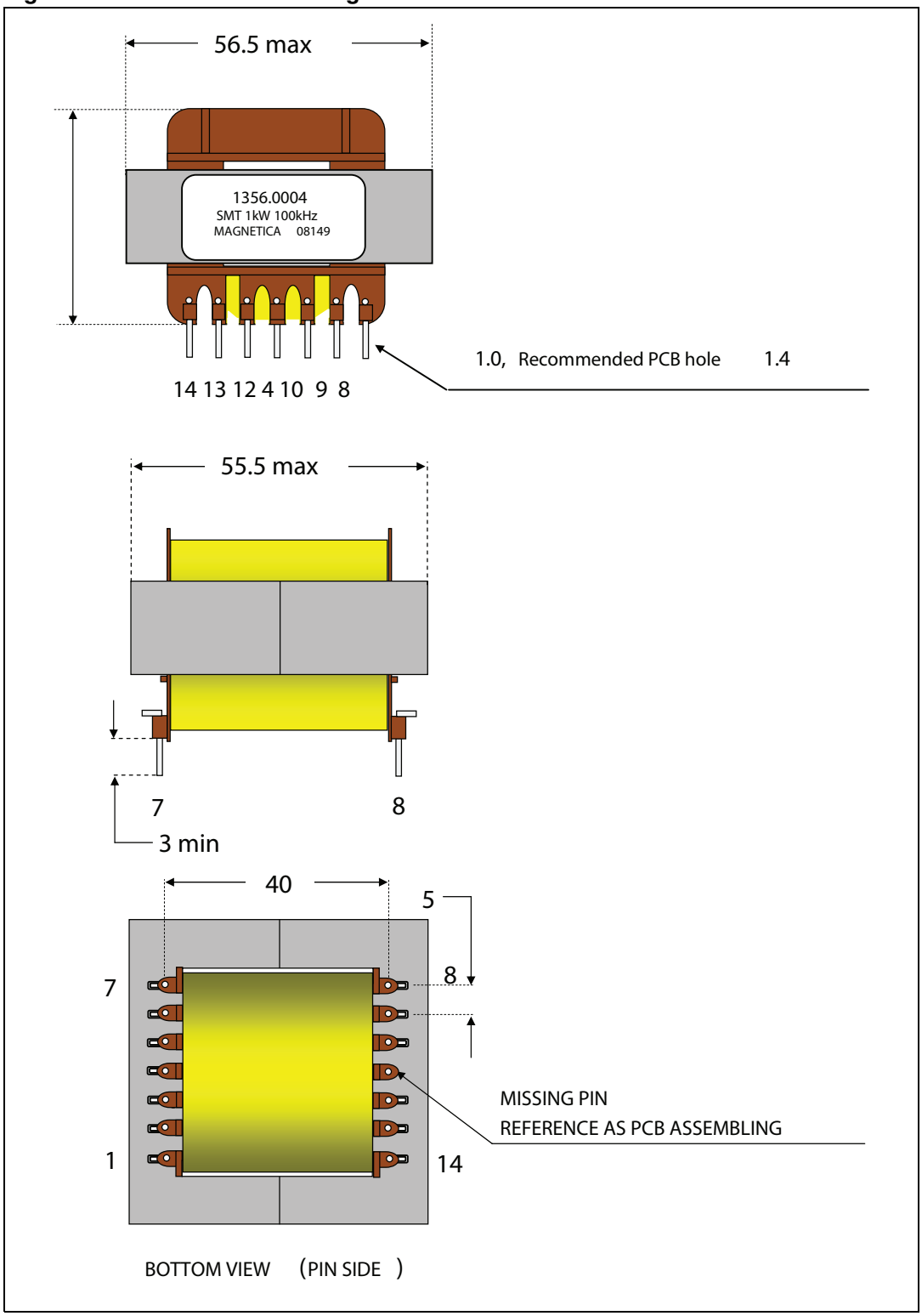

7 Revision history

Table 8. Document revision history

Date	Revision	Changes
16-Feb-2009	1	Initial release
13-Jan-2012	2	– Introduction modified – *Section 3* modified

Please Read Carefully:

Information in this document is provided solely in connection with ST products. STMicroelectronics NV and its subsidiaries (“ST”) reserve the right to make changes, corrections, modifications or improvements, to this document, and the products and services described herein at any time, without notice.

All ST products are sold pursuant to ST’s terms and conditions of sale.

Purchasers are solely responsible for the choice, selection and use of the ST products and services described herein, and ST assumes no liability whatsoever relating to the choice, selection or use of the ST products and services described herein.

No license, express or implied, by estoppel or otherwise, to any intellectual property rights is granted under this document. If any part of this document refers to any third party products or services it shall not be deemed a license grant by ST for the use of such third party products or services, or any intellectual property contained therein or considered as a warranty covering the use in any manner whatsoever of such third party products or services or any intellectual property contained therein.

UNLESS OTHERWISE SET FORTH IN ST’S TERMS AND CONDITIONS OF SALE ST DISCLAIMS ANY EXPRESS OR IMPLIED WARRANTY WITH RESPECT TO THE USE AND/OR SALE OF ST PRODUCTS INCLUDING WITHOUT LIMITATION IMPLIED WARRANTIES OF MERCHANTABILITY, FITNESS FOR A PARTICULAR PURPOSE (AND THEIR EQUIVALENTS UNDER THE LAWS OF ANY JURISDICTION), OR INFRINGEMENT OF ANY PATENT, COPYRIGHT OR OTHER INTELLECTUAL PROPERTY RIGHT.

UNLESS EXPRESSLY APPROVED IN WRITING BY TWO AUTHORIZED ST REPRESENTATIVES, ST PRODUCTS ARE NOT RECOMMENDED, AUTHORIZED OR WARRANTED FOR USE IN MILITARY, AIR CRAFT, SPACE, LIFE SAVING, OR LIFE SUSTAINING APPLICATIONS, NOR IN PRODUCTS OR SYSTEMS WHERE FAILURE OR MALFUNCTION MAY RESULT IN PERSONAL INJURY, DEATH, OR SEVERE PROPERTY OR ENVIRONMENTAL DAMAGE. ST PRODUCTS WHICH ARE NOT SPECIFIED AS "AUTOMOTIVE GRADE" MAY ONLY BE USED IN AUTOMOTIVE APPLICATIONS AT USER’S OWN RISK.

Resale of ST products with provisions different from the statements and/or technical features set forth in this document shall immediately void any warranty granted by ST for the ST product or service described herein and shall not create or extend in any manner whatsoever, any liability of ST.

ST and the ST logo are trademarks or registered trademarks of ST in various countries.

Information in this document supersedes and replaces all information previously supplied.

The ST logo is a registered trademark of STMicroelectronics. All other names are the property of their respective owners.

© 2012 STMicroelectronics - All rights reserved

STMicroelectronics group of companies

Australia - Belgium - Brazil - Canada - China - Czech Republic - Finland - France - Germany - Hong Kong - India - Israel - Italy - Japan - Malaysia - Malta - Morocco - Philippines - Singapore - Spain - Sweden - Switzerland - United Kingdom - United States of America

www.st.com